

N72-32939

NASA TECHNICAL NOTE



NASA TN D-6966

NASA TN D-6966

CASE FILE
COPY

CORRELATION FOR TEMPERATURE PROFILES
IN THE PLANE OF SYMMETRY DOWNSTREAM
OF A JET INJECTED NORMAL TO A CROSSFLOW

by James D. Holdeman

Lewis Research Center
Cleveland, Ohio 44135

NATIONAL AERONAUTICS AND SPACE ADMINISTRATION • WASHINGTON, D. C. • SEPTEMBER 1972

1. Report No. NASA TN D-6966	2. Government Accession No.	3. Recipient's Catalog No.	
4. Title and Subtitle CORRELATION FOR TEMPERATURE PROFILES IN THE PLANE OF SYMMETRY DOWNSTREAM OF A JET INJECTED NORMAL TO A CROSSFLOW		5. Report Date September 1972	
7. Author(s) James D. Holdeman		6. Performing Organization Code	
9. Performing Organization Name and Address Lewis Research Center National Aeronautics and Space Administration Cleveland, Ohio 44135		8. Performing Organization Report No. E-6860	
12. Sponsoring Agency Name and Address National Aeronautics and Space Administration Washington, D.C. 20546		10. Work Unit No. 764-74	
15. Supplementary Notes		11. Contract or Grant No.	
		13. Type of Report and Period Covered Technical Note	
		14. Sponsoring Agency Code	
16. Abstract <p>A correlation method is presented for approximating the temperature distribution in the plane of symmetry downstream of a jet injected normal to a uniform crossflow. Correlations are developed for the scaling parameters required to define the temperature profile at any desired location from the dimensionless universal form which has been experimentally observed. Profiles calculated using the correlation method are compared with experimental profiles for several momentum and density ratios at various downstream distances.</p>			
17. Key Words (Suggested by Author(s)) Turbulent jets; Crossflow; Temperature distribution; Dilution jet mixing; Combustion gas dilution		18. Distribution Statement Unclassified - unlimited	
19. Security Classif. (of this report) Unclassified	20. Security Classif. (of this page) Unclassified	21. No. of Pages 28	22. Price* \$3.00

* For sale by the National Technical Information Service, Springfield, Virginia 22151

CORRELATION FOR TEMPERATURE PROFILES IN THE PLANE OF SYMMETRY DOWNSTREAM OF A JET INJECTED NORMAL TO A CROSSFLOW

by James D. Holdeman

Lewis Research Center

SUMMARY

A correlation method is presented for approximating the temperature distribution in the plane of symmetry downstream of a jet injected perpendicularly to a uniform, unbounded crossflow. The method is based on the experimental observation that for the proper selection of scaling parameters, the dimensionless temperature profiles can be expressed in a self-similar form. With the profile shape defined, the temperature distribution in the plane of symmetry at any downstream location can be determined from the correlations presented for the temperature centerline location and the scaling parameters in terms of the initial jet-to-crossflow momentum and density ratios and the downstream distance. Calculated profiles are compared with experimental results for several momentum and density ratios at varying downstream distances.

INTRODUCTION

The injection of a single jet into a semi-infinite crossflow may be viewed as a basic component of the complex flow in the dilution zone of gas turbine combustion chambers. In this report a correlation method is presented for approximating the temperature distribution in the plane of symmetry downstream of a jet directed perpendicularly to a crossflow.

In a typical gas turbine combustor, from 30 to 60 percent of the total airflow enters the chamber downstream of the primary zone and must be mixed in the dilution zone with the high temperature combustion gases to provide a suitable temperature distribution at the turbine inlet. Rapid mixing within a short length can be achieved with jets which penetrate from the combustor liner walls into the hot gas stream. As the jets are deflected by the mainstream flow, the production of streamwise vorticity establishes twin secondary motions within each jet which cause large scale mixing.

In recent years, considerable attention has been given to various aspects of the jet in a subsonic crossflow problem because it is the basic configuration in several problems of current technological importance. The most notable of these, in addition to the combustor dilution mixing problem, are (1) film and impingement cooling of turbine blades, (2) the aerodynamic effect on a VTOL or STOL aircraft caused by the jet flow from a lifting propulsion system, and (3) the pollutant concentration downwind from a chimney.

Results relevant to combustion gas dilution cannot generally be extrapolated from studies which are addressed primarily to the other problems, although some parameters, such as the jet trajectory are of common interest. Based on the published studies which preceded the present work, the extant information relevant to the diffusion of heat and momentum downstream of a jet injected normal to a crossflow can be summarized as follows:

(1) The trajectory of a single jet injected normal to an unbounded crossflow has been reported in references 1 to 5.

(2) Centerplane temperature profile results downstream of a heated sonic jet injected into a subsonic crossflow in a narrow wind tunnel have been presented in references 6 and 7.

(3) Temperature profiles downstream of opposing rows of jets were found to be dependent on the jet to mainstream mass flux ratios in reference 8.

(4) Based on data in references 9 and 10, for the temperature field downstream of a single heated jet injected normal to a crossflow at low momentum ratios, a model for the temperature field has been proposed in reference 11.

(5) The decay of the maximum temperature and the spread of a jet in a crossflow as a function of distance along the jet trajectory were examined in references 4 and 5.

(6) Transverse distributions of temperature in the plane of symmetry are shown in references 4 and 5 to be expressible in a self-similar form.

In the present report, the observed self-similar form of the nondimensionalized centerplane temperature profiles is used as the basis for predicting the centerplane temperature distribution at a specified distance downstream from the injection location. To define the temperature distribution from the nondimensional form, it is necessary to know the location of the temperature centerline and the values of the scaling parameters which appear in the dimensionless form. For the present problem these are the magnitude of the maximum temperature difference at the centerline and the displacements from the centerline at which the temperature difference is one half of the value at the centerline. These parameters are correlated as functions of the jet-to-crossflow density and momentum ratio and the distance downstream from the jet injection location. Unless otherwise indicated, the experimental data shown in this report are from the study of reference 4, obtained under NASA Grant NGR 36-027-008.

TRAJECTORY AND PROFILE SHAPE RESULTS FROM PREVIOUS INVESTIGATIONS

The flow field in the vicinity of a jet injected normal to a crossflow is shown schematically in figure 1. The most frequently reported characteristic of the flow is the jet trajectory, defined as a function of downstream distance by the perpendicular displacement from the wall ($Z = 0$) to the location of the local maximum centerplane velocity. Several previous investigations which have provided a basis for predicting the jet trajectory are cited in references 1 to 4. The following empirical relation for the trajectory from reference 4 is based on several momentum ratios (obtained with various density and velocity combinations):

$$\frac{Z_v}{D} = 0.89 J^{0.47} \left(\frac{X}{D} \right)^{0.36} \quad (1)$$

where $J \equiv (\rho_j V_j^2) / (\rho_\infty U_\infty^2)$. (All symbols are defined in appendix A.) Experimental results from reference 5 indicating the effect of various initial conditions on the trajectory, experimental results of Keffer and Baines (ref. 12), and calculated values of the trajectory for $J = 18$ based on relations obtained by Margason (ref. 2), Ivanov (from Abramovich, ref. 3), and Jordinson (ref. 13) are shown in figure 2, as is equation (1). Although the reported exponents vary between the several empirical expressions, they are of the same form as equation (1). As the data from reference 5 indicate, trajectory differences are most likely the result of different initial conditions on the jet and crossflow, that is, varying thickness of the wall boundary layer at the injection point and varying jet velocity profiles. The most important conclusion from the velocity trajectory measurements is that the trajectory can be correlated based on momentum ratio and distance alone.

Recently, the results of experimental studies of the complete temperature distribution downstream from a single heated jet injected normal to an ambient temperature crossflow have been reported by Ramsey and Goldstein (refs. 9 and 10) and Kamotani and Greber (refs. 4 and 5). Because the study of Ramsey and Goldstein was for film cooling applications, the momentum ratios considered were considerably smaller than those examined in reference 4, which was motivated by the dilution jet mixing problem.

Based on the experimental results in references 9 and 10, a model for the temperature field downstream of the jet injection point has been proposed by Erickson, Eckert, and Goldstein (ref. 11). This model assumes that the temperature distribution downstream of a jet in a crossflow is analogous to the temperature field formed by a moving point source of heat in a solid. The Gaussian solution thus generated agrees satisfactorily with the experimental results for low momentum ratios, where the maximum

temperature difference at all downstream locations is at an approximately constant distance from the wall. This model is not applicable to the larger momentum ratios characteristic of dilution jet mixing due to the significant increase in the height of the trajectory with increasing downstream distance.

Temperature distributions were measured by Kamotani and Greber (ref. 4) in planes normal to the velocity trajectory. A section of the flow field through the center-plane (X, Z-plane, see fig. 1), showing the orientation of the measurement planes and the scaling parameters necessary to describe the temperature distributions is shown schematically in figure 3. Transverse distributions of temperature, as indicated by the profile in figure 3, were found to be expressible in a self-similar form which can be approximated by a Gaussian distribution; that is,

$$\frac{\theta}{\theta_c} = \exp \left[- \ln 2 \left(\frac{\frac{L}{D}}{\frac{L_{1/2}^+}{D} + \frac{L_{1/2}^-}{D}} \right)^2 \right] \quad (2)$$

where $\theta = \theta_c$ at the temperature centerline (Z_c/D) and θ_c , $L_{1/2}^+/D$, and $L_{1/2}^-/D$ are scaling parameters. Equation (2) and the data from reference 4 are shown in figure 4.

CORRELATIONS REQUIRED TO DEFINE THE CENTERPLANE TEMPERATURE DISTRIBUTIONS

The scaling parameters θ_c , $L_{1/2}^+/D$, and $L_{1/2}^-/D$ in the self-similar, dimensionless temperature distributions given by equation (2) have not been related to the geometric and initial flow conditions of the problem in previous studies. In this report, data from the study of reference 4 is used to establish correlations for the scaling parameters in terms of the initial ratios of jet-to-crossflow momentum and density and the downstream distance. The relations obtained are of the following form:

$$f = c \left(\frac{\rho_j}{\rho_\infty} \right)^a J^b \left(\frac{X}{D} \right)^d$$

where f may be Z_c/D , θ_c , $L_{1/2}^+/D$ or $L_{1/2}^-/D$ and c , a , b , and d are constants. When used with equation (2), these correlations provide a method for approximating the

centerplane temperature profile at any location downstream of the injection point when the initial conditions are known.

In the following paragraphs the required correlations, namely, (1) Z_c/D , the jet centerline defined by the location of the local maximum temperature difference; (2) θ_c , the local maximum temperature difference ratio; and (3) $L_{1/2}^+/D$ and $L_{1/2}^-/D$, the displacements from the centerline at which the temperature difference ratio is equal to $\theta_c/2$, are presented. These parameters are shown in figure 3.

In the nonisothermal flow field, a jet temperature centerline exists which is not coincident with the velocity trajectory, equation (1). The temperature centerline, like the velocity trajectory is mainly dependent on momentum ratio and distance. It is shown in reference 5 that the temperature centerline is weakly dependent on density ratio also. Based on data for momentum ratios in the range $15 < J < 60$, the temperature centerline may be described by the following relation:

$$\frac{Z_c}{D} = 0.76 \left(\frac{\rho_j}{\rho_\infty} \right)^{0.15} J^{0.52} \left(\frac{X}{D} \right)^{0.27} \quad (3)$$

The agreement between the data and the correlation equation is shown in figure 5. It should be noted that the centerline data from reference 9 are also correlated satisfactorily by this relation.

The correlation for the temperature decay along the centerline is described by the following relation:

$$\theta_c = 1.85 \left(\frac{\rho_j}{\rho_\infty} \right)^{0.71} J^{-0.43} \left(\frac{X}{D} \right)^{-0.63} \quad (4)$$

where

$$\theta_c = \frac{T - T_\infty}{T_j - T_\infty}$$

The centerline temperature decay shows a stronger dependence on the density ratio than does the centerline location. Equation (4) and the experimental data from which it was determined are shown in figure 6. Centerline temperature decay data from reference 9, for momentum ratios $J < 5$ are also shown. These data (ref. 9) are consistently slightly below the correlation curve.

In addition to the θ_c and Z_c/D correlations discussed previously, specification of the centerplane temperature profiles requires expressions for the spread of the temperature distribution. This is described by the temperature profile half-widths, $L_{1/2}^+/D$ and $L_{1/2}^-/D$, defined as the displacements from the temperature centerline at which the temperature difference ratio is equal to $\theta_c/2$. The following relations for the temperature field spread rate were determined from the temperature profile data obtained in the study of reference 4:

$$\frac{L_{1/2}^+}{D} = 0.33 J^{0.28} \left(\frac{X}{D}\right)^{0.38} \quad (5)$$

$$\frac{L_{1/2}^-}{D} = 0.61 J^{0.25} \left(\frac{X}{D}\right)^{0.28} \quad (6)$$

A density ratio factor is not included in these correlations because no consistent variation of the half-widths as a function of density ratio was apparent from the data. Because the half-width for the profile above the centerline is not the same as the half-width for the profile below the centerline, the temperature distribution is asymmetric. This is in contrast to the symmetric distribution which would be predicted by the method of reference 11.

For the combustor dilution mixing application, it is more convenient to have the centerplane temperature distribution expressed in planes normal to the undisturbed crossflow. If a Gaussian distribution is assumed in these planes, then at any desired downstream location the vertical centerplane temperature profile is defined by correlations of θ_c , Z_c/D , and $H_{1/2}^+/D$ and $H_{1/2}^-/D$, where $H_{1/2}^+/D$ and $H_{1/2}^-/D$ are the vertical displacements (half-heights) from the centerline to where $\theta = \theta_c/2$ (see fig. 7). The relation between vertical temperature profiles and profiles in planes normal to the jet trajectory is derived in appendix B.

The experimental data for $L_{1/2}^+/D$ and $L_{1/2}^-/D$, the correlation equations (5) and (6), and half-heights calculated for the two principal momentum ratios examined experimentally by Kamotani and Greber are shown in figure 8. The half-heights are always less than $(L_{1/2}^{\pm}/D)/\cos \varphi$ where $\tan \varphi = dZ_v/dX$ and are greater than the half-widths by less than 10 percent for $\varphi \leq 30^{\circ}$.

COMPARISON OF CALCULATED AND EXPERIMENTAL RESULTS

The correlation of the various scaling parameters with the flow and geometric parameters presented in the preceding section provides a method for approximating the

centerplane temperature profiles downstream of a jet injected perpendicularly to a uniform crossflow. Several profiles have been calculated based on experimental conditions in references 4 and 9 and are compared with the experimental results in figures 9 to 15.

Typical centerplane temperature profiles obtained in planes normal to the velocity trajectory (fig. 3) are shown in figure 9. Calculated profiles are compared with the experimental data at several downstream distances. The angle between the measurement plane and the vertical axis φ is indicated on figure 9. The agreement between the calculated and experimental profiles is very good, especially for $\varphi < 40^\circ$. Because the inclination of the data planes is a variable, these profiles are shown as θ plotted against L/D .

The suitability of the correlation method for approximating temperature profiles measured in vertical planes (fig. 7) is shown in figures 10 to 15. These profiles are presented as θ plotted against Z/D , and thus indicate the overall accuracy of the correlation method as the calculated profiles shown depend on Z_c/D , θ_c , and $H_{1/2}^\pm/D$. For the calculations, the $L_{1/2}^+/D$ and $L_{1/2}^-/D$ correlations were used to approximate the half-heights.

Figures 10, 11, and 12 show calculated and experimental profiles at a momentum ratio J of 15.3 for density ratios in the range $0.625 \leq \rho_j/\rho_\infty \leq 0.877$ at downstream distances $10 \leq X/D \leq 50$. Experimental profiles at several downstream distances for $J = 59.6$ and $\rho_j/\rho_\infty = 0.625$ are shown with the calculated profiles in figure 13. The agreement between calculated and experimental profiles is very good for all cases.

Vertical centerplane temperature profiles from reference 9 are shown in figures 14 and 15. Although the momentum ratios investigated in these experiments were much less than the momentum ratios of the data on which the correlations are based, satisfactory agreement between calculated and experimental profiles is achieved. The deviations between the experimental data and the calculated profile apparent at $X/D = 1.87$ are not unexpected as a separated flow region is known to exist in the near region downstream of the jet as shown by the tuft measurements of reference 9. Thus the Gaussian profile assumption is a tenuous one in this region; however, with respect to the upper half of the profile, the calculated curve does provide a good approximation to the data. The analytical profiles in reference 11 for a momentum ratio of 4.74 are shown in figure 14. The profiles calculated using the method of this report, provide a better approximation to the data than does the model of reference 11 because, in the present method, the temperature centerline is not held constant with respect to distance, and asymmetry of the profiles is assumed.

If the complete description of the temperature profiles as shown in the preceding paragraphs is not required, a composite representation of the location and spreading characteristics of the temperature field can be obtained by considering the locus of points where $\theta = \theta_c/2$ thereby defining upper and lower half-width trajectories, $Z_{1/2}^+/D$

and $Z_{1/2}^+/D$ (see fig. 3). Based on the correlations of θ_c , Z_c/D , and $L_{1/2}^+/D$ given previously, the half-width trajectories can be calculated, or they may be determined from the following relations which provide an excellent approximation:

$$\frac{Z_{1/2}^+}{D} = 1.03 \left(\frac{\rho_j}{\rho_\infty} \right)^{0.1} J^{0.47} \left(\frac{X}{D} + 0.5 \right)^{0.3} \quad (7)$$

$$\frac{Z_{1/2}^-}{D} = 0.35 \left(\frac{\rho_j}{\rho_\infty} \right)^{0.2} J^{0.65} \left(\frac{X}{D} - 0.5 \right)^{0.25} \quad (8)$$

Half-width trajectories, temperature centerlines, and velocity trajectories calculated for $J = 10$, 40 , and 70 are shown superimposed on smoke photographs in figure 16. The location of the velocity trajectory on these figures indicates that the smoke is a velocity field tracer, as was intended. The temperature centerline and the half-width trajectories show the location and relative width of the temperature field. These appear slightly low with respect to the velocity field as expected.

SUMMARY OF RESULTS

A method is presented for predicting the centerplane temperature distribution downstream of a jet injected normal to a uniform crossflow. The method is based on the experimental observation that the properly nondimensionalized centerplane temperature profiles may be expressed as

$$\theta = \theta_c \exp \left[- \ln 2 \left(\frac{\frac{L}{D}}{\frac{L_{1/2}^+}{D}} \right)^2 \right]$$

where θ is the temperature difference ratio $(T - T_\infty)/(T_j - T_\infty)$, θ_c is the temperature difference ratio at the centerline, L/D is the distance from the temperature centerline, and $L_{1/2}^+/D$ are the temperature profile half-widths. Thus the temperature profile at any desired downstream location can be determined from the correlations presented in this report for (1) Z_c/D , the jet temperature centerline, (2) θ_c , and (3) $L_{1/2}^+/D$ and

$L_{1/2}/D$. Profiles calculated using the correlation method are shown to agree very well with experimental data for a wide range of momentum ratios.

Lewis Research Center,
National Aeronautics and Space Administration,
Cleveland, Ohio, June 26, 1972,
764-74.

APPENDIX A

SYMBOLS

D	jet diameter
$H_{1/2}^{\pm}$	vertical distance from temperature centerline to where $\theta = \theta_c/2$
J	jet to free stream momentum ratio, $\rho_j V_j^2 / \rho_{\infty} U_{\infty}^2$
L	displacement from temperature centerline in planes normal to velocity trajectory
$L_{1/2}^{\pm}$	displacements from temperature centerline to where $\theta = \theta_c/2$ in planes normal to velocity trajectory (see eqs. (5) and (6))
T	temperature
U	velocity in direction of coordinate X
V	velocity in direction of coordinate Z
X	streamwise coordinate (see fig. 1)
Y	lateral coordinate (see fig. 1)
Z	vertical coordinate (see fig. 1)
Z_c	location of local maximum centerplane temperature difference (see eq. (3))
Z_v	location of local maximum centerplane velocity (see eq. (1))
$Z_{1/2}^{\pm}$	vertical distance to where $\theta = \theta_c/2$ (see eqs. (7) and (8))
θ	temperature difference ratio, $(T - T_{\infty}) / (T_j - T_{\infty})$ (see eq. (2))
θ_c	temperature difference ratio at points along temperature centerline (see eq. (4))
ρ	fluid density
φ	inclination of velocity trajectory from horizontal plane

Subscripts:

c	refers to temperature centerline
i	refers to point where $\theta = \theta_c/2$ for upper profile (see appendix B)
j	jet exit condition
k	refers to point where $\theta = \theta_c/2$ for the lower profile (see appendix B)
v	refers to velocity trajectory
∞	undisturbed crossflow condition

Superscripts:

- + refers to upper profile
- refers to lower profile

APPENDIX B

RELATION BETWEEN VERTICAL TEMPERATURE PROFILES AND PROFILES IN PLANES NORMAL TO THE JET TRAJECTORY

The relation between vertical temperature profiles and temperature profiles in planes normal to the velocity trajectory can be determined from the following empirical relations:

Velocity trajectory:

$$\frac{z_v}{D} = 0.89 J^{0.47} \left(\frac{x_v}{D} \right)^{0.36} \quad (B1)$$

Temperature centerline:

$$\frac{z_c}{D} = 0.76 \left(\frac{\rho_j}{\rho_\infty} \right)^{0.15} J^{0.52} \left(\frac{x_c}{D} \right)^{0.27} \quad (B2)$$

Centerline temperature difference ratio:

$$\theta_c = 1.85 \left(\frac{\rho_j}{\rho_\infty} \right)^{0.71} J^{-0.43} \left(\frac{x}{D} \right)^{-0.63} \quad (B3)$$

Temperature profile half-widths:

$$\left. \frac{L_{1/2}^+}{D} \right|_{X=X_c} = 0.33 J^{0.28} \left(\frac{x_c}{D} \right)^{0.38} \quad (B4)$$

$$\left. \frac{L_{1/2}^-}{D} \right|_{X=X_c} = 0.61 J^{0.25} \left(\frac{x_c}{D} \right)^{0.28} \quad (B5)$$

$$\frac{d\left(\frac{Z_v}{D}\right)}{d\left(\frac{X_v}{D}\right)} = \tan \varphi = 0.36 \frac{\frac{Z_v}{D}}{\frac{X_v}{D}} \quad (B6)$$

From figure 17, it can be seen that

$$\frac{\frac{X_c}{D} - \frac{X_v}{D}}{\frac{Z_v}{D} - \frac{Z_c}{D}} = \tan \varphi = 0.36 \frac{\frac{Z_v}{D}}{\frac{X_v}{D}} \quad (B7)$$

Substituting for Z_v/D and Z_c/D gives

$$0.89 J^{0.47} \left(\frac{X_v}{D}\right)^{0.36} = 0.76 \left(\frac{\rho_j}{\rho_\infty}\right)^{0.15} J^{0.52} \left(\frac{X_c}{D}\right)^{0.27} + \frac{\left(\frac{X_v}{D}\right)^{0.64}}{(0.36)(0.89)J^{0.47}} \left(\frac{X_c}{D} - \frac{X_v}{D}\right) \quad (B8)$$

which can be solved iteratively for X_c/D , and Z_c/D ; then, θ_c can be determined from equation (B3).

For the upper profile, $\theta_i = \theta_c/2$ at

$$\frac{Z_i}{D} = \frac{Z_c}{D} + \frac{L_{1/2}^+}{D} \Bigg|_{X=X_c} \cos \varphi \quad (B9)$$

$$\frac{X_i}{D} = \frac{X_c}{D} - \frac{L_{1/2}^+}{D} \Bigg|_{X=X_c} \sin \varphi \quad (B10)$$

At X_i/D , the centerline values are $\theta_{c,i}$ and $Z_{c,i}/D$. Assuming the vertical profile at X_i/D can be described by a Gaussian distribution, we have

$$\theta_i = \theta_{c,i} \exp \left[-\ln 2 \left(\frac{\frac{Z_i}{D} - \frac{Z_{c,i}}{D}}{\frac{H_{1/2}^+}{D}} \right)^2 \right] \quad (B11)$$

Since $\theta_i = \theta_c/2$, $H_{1/2}^+ / D \Big|_{X=X_i}$ is given by

$$\frac{H_{1/2}^+}{D} \Big|_{X=X_i} = \left(\frac{Z_i}{D} - \frac{Z_{c,i}}{D} \right) \sqrt{\frac{\ln 2}{\ln \frac{2\theta_{c,i}}{\theta_c}}} \quad (B12)$$

This can be compared with the upper half-width at X_i/D which is given by

$$\frac{L_{1/2}^+}{D} \Big|_{X=X_i} = 0.33 J^{0.28} \left(\frac{X_i}{D} \right)^{0.38} \quad (B13)$$

Similarly, for the lower profile $\theta_k = \theta_c/2$ at

$$\frac{Z_k}{D} = \frac{Z_c}{D} - \frac{L_{1/2}^-}{D} \Big|_{X=X_c} \cos \varphi \quad (B14)$$

$$\frac{X_k}{D} = \frac{X_c}{D} + \frac{L_{1/2}^-}{D} \Big|_{X=X_c} \sin \varphi \quad (B15)$$

At X_k/D , the centerline values are $\theta_{c,k}$ and $Z_{c,k}/D$. Assuming the vertical profile at X_k/D can be described by a Gaussian distribution, the lower half-height is given by

$$\left. \frac{H_{1/2}}{D} \right|_{X=X_c} = \left(\frac{Z_{c,k}}{D} - \frac{Z_k}{D} \right) \sqrt{\frac{\ln 2}{\ln \frac{2\theta_{c,k}}{\theta_c}}} \quad (B16)$$

which can be compared with the lower half-width at X_k/D which is given by

$$\left. \frac{L_{1/2}}{D} \right|_{X=X_c} = 0.61 J^{0.25} \left(\frac{X_c}{D} \right)^{0.28} \quad (B17)$$

REFERENCES

1. Anon.: Analysis of a Jet in a Subsonic Crosswind. NASA SP-218, 1969.
2. Margason, Richard J.: The Path of a Jet Directed at Large Angles to a Subsonic Free Stream. NASA TN D-4919, 1968.
3. Abramovich, G. N.: The Theory of Turbulent Jets. MIT Press, 1963.
4. Kamotani, Yasuhiro; and Greber, Isaac: Experiments on a Turbulent Jet in a Cross Flow. Rep. FTAS/TR-71-62, Case Western Reserve Univ. (NASA CR-72893), June 1971.
5. Kamotani, Y.; and Greber, I.: Experiments on a Turbulent Jet in a Cross Flow. Paper 72-149, AIAA, Jan. 1972.
6. Callaghan, Edmund E.; and Ruggeri, Robert S.: Investigation of the Penetration of an Air Jet Directed Perpendicularly to an Air Stream. NACA TN 1615, 1948.
7. Callaghan, Edmund E.; and Ruggeri, Robert S.: A General Correlation of Temperature Profiles Downstream of a Heated-Air Jet Directed Perpendicularly to an Air Stream. NACA TN 2466, 1951.
8. Norgren, Carl T.; and Humenik, Francis M.: Dilution-Jet Mixing Study for Gas-Turbine Combustors. NASA TN D-4695, 1968.
9. Ramsey, J. W.; and Goldstein, R. J.: Interaction of a Heated Jet with a Deflecting Stream. Rep. HTL-TR-92, Minnesota Univ. (NASA CR-72613), Apr. 1970.
10. Ramsey, J. W.; and Goldstein, R. J.: Interaction of a Heated Jet with a Deflecting Stream. Paper 71-HT-2, ASME, Aug. 1971.
11. Eriksen, V. L.; Eckert, E. R. G.; and Goldstein, R. J.: A Model for Analysis of the Temperature Field Downstream of a Heated Jet Injected into an Isothermal Crossflow at an Angle of 90°. Rep. HTL-TR-101, Minnesota Univ. (NASA CR-72990), July 1971.
12. Keffer, J. F.; and Baines, W. D.: The Round Turbulent Jet in a Cross-Wind. J. Fluid Mech., vol. 15, pt. 4, Apr. 1963, pp. 481-496.
13. Jordinson, R.: Flow in a Jet Directed Normal to the Wind. R & M 3074, Aeronautical Research Council, Great Britain, 1958.

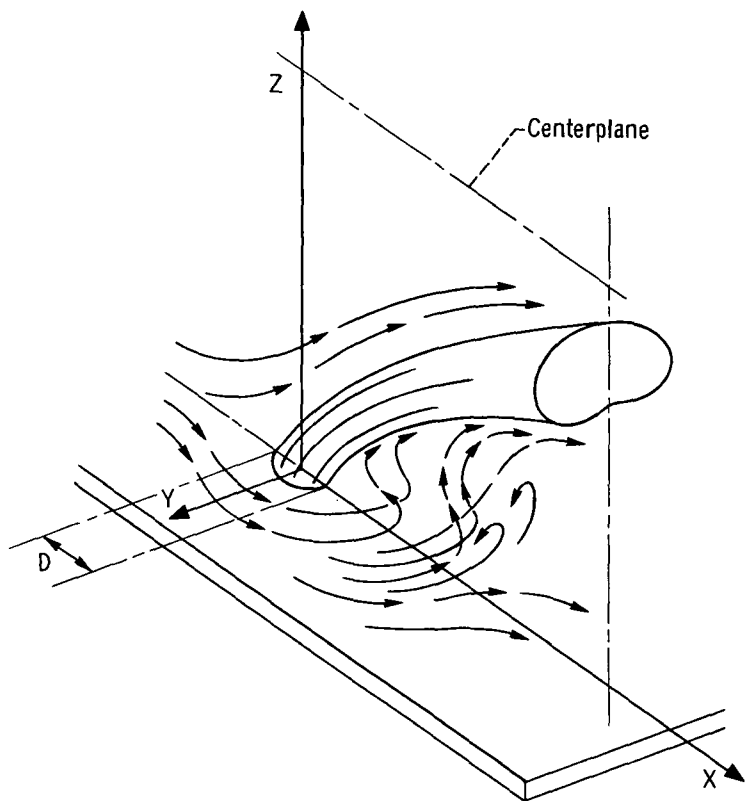


Figure 1. - Jet in crossflow.

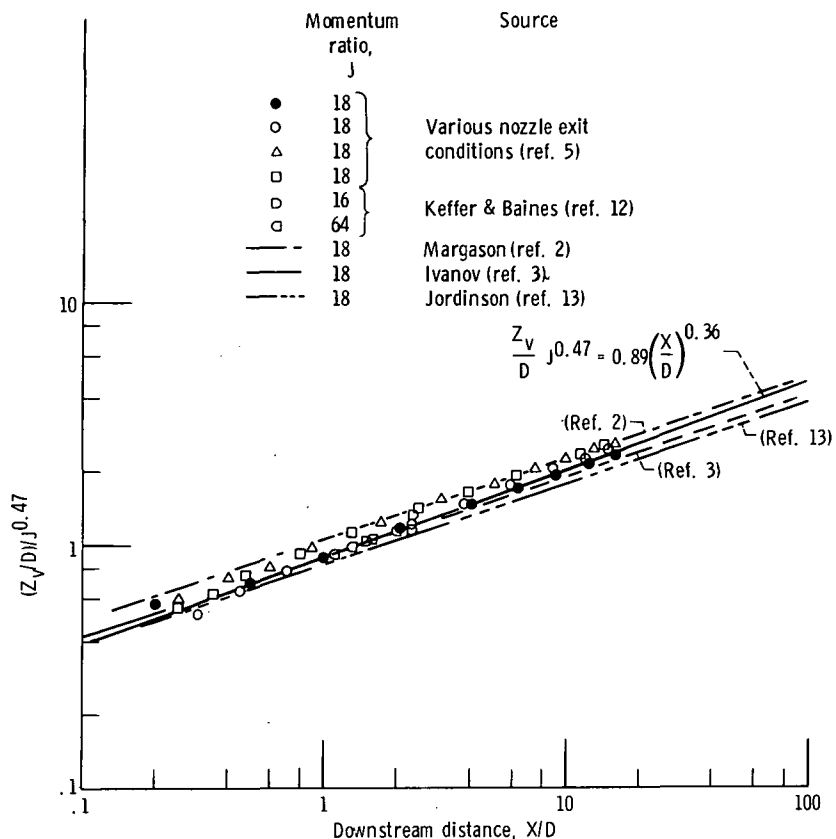


Figure 2. - Correlation of velocity trajectory data from several investigations.

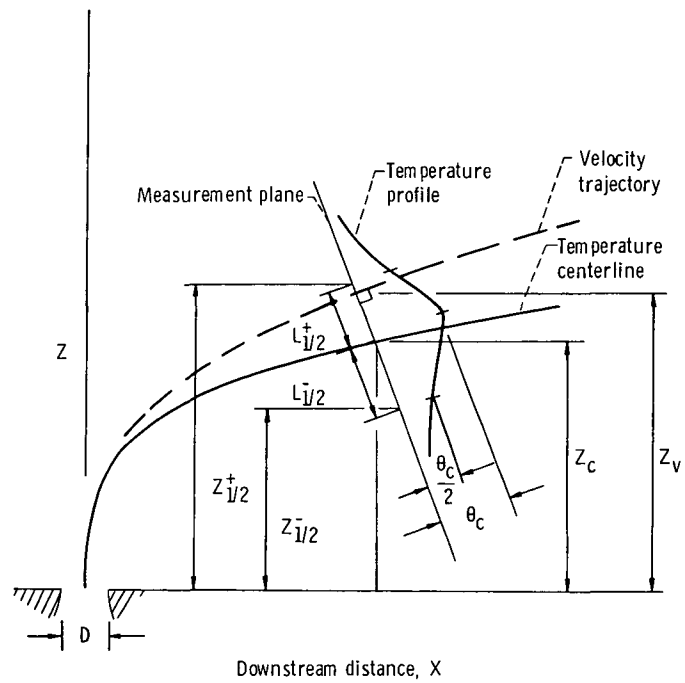


Figure 3. - Coordinates for temperature profiles normal to velocity trajectory.

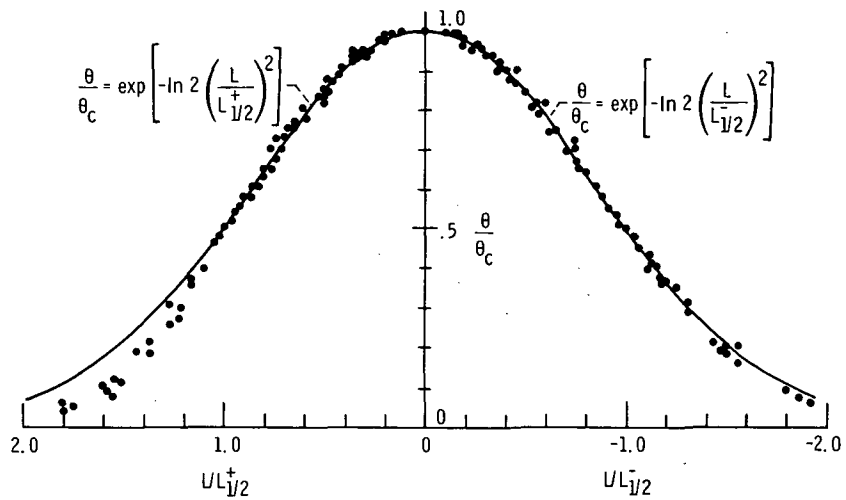


Figure 4. - Nondimensional centerplane temperature profile in planes normal to velocity trajectory (from ref. 4).

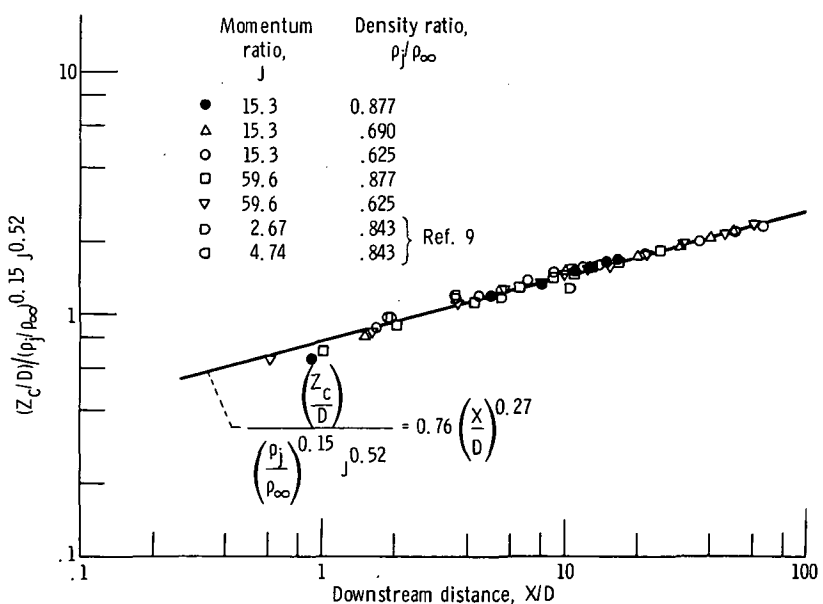


Figure 5. - Correlation of temperature centerline data for various momentum ratios J and density ratios p_j / p_∞ .

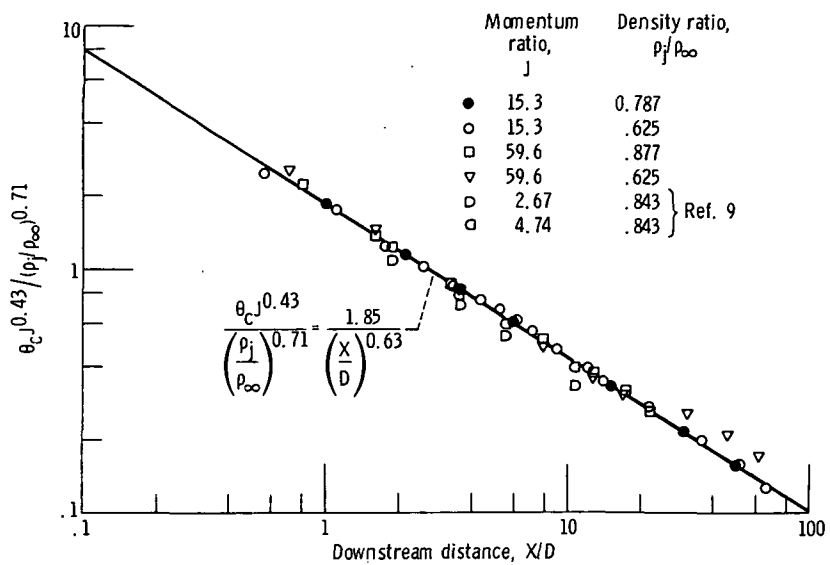


Figure 6. - Correlation of centerline temperature data for various momentum ratios J and density ratios ρ_j/ρ_∞ .

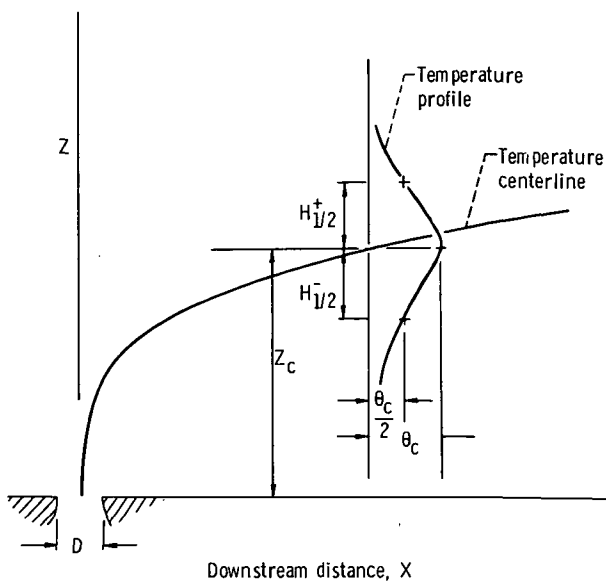


Figure 7. - Coordinates for centerplane temperature profiles in vertical planes.

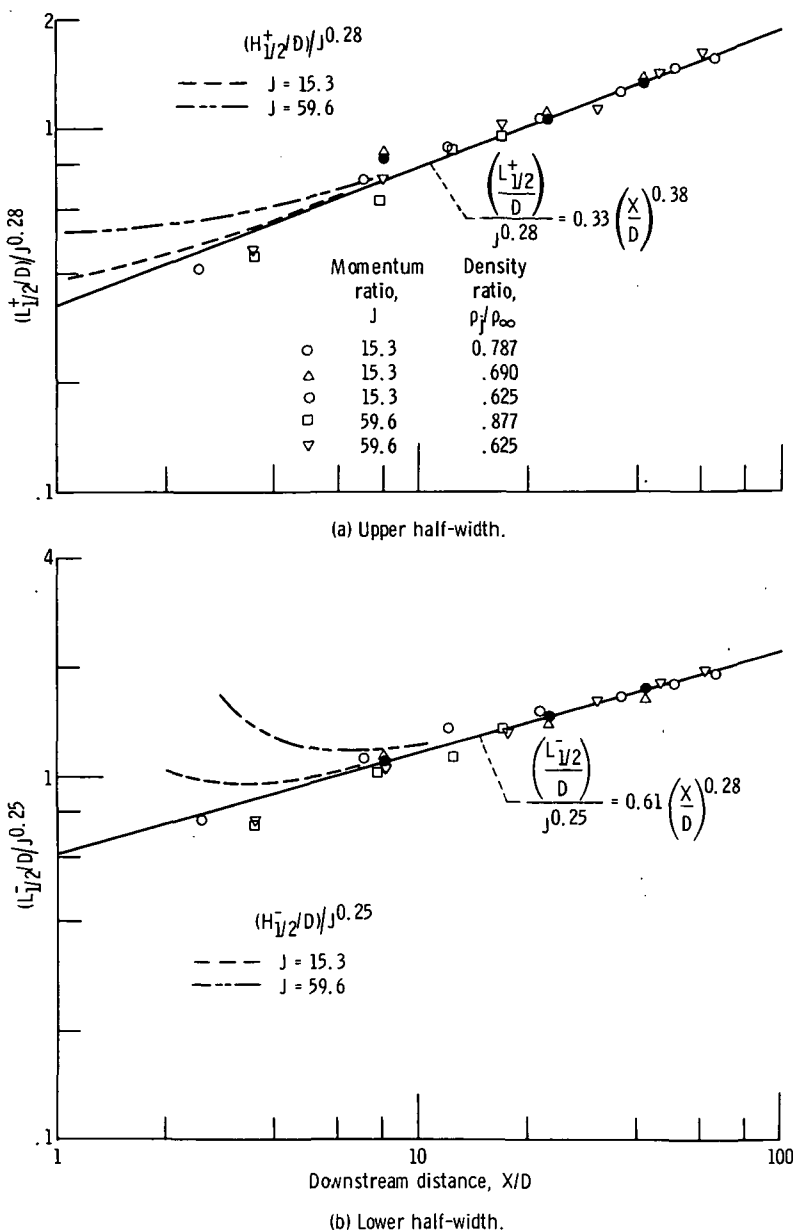


Figure 8. - Correlation of temperature profile half-width data for various momentum ratios J and density ratios ρ_J/ρ_∞ .

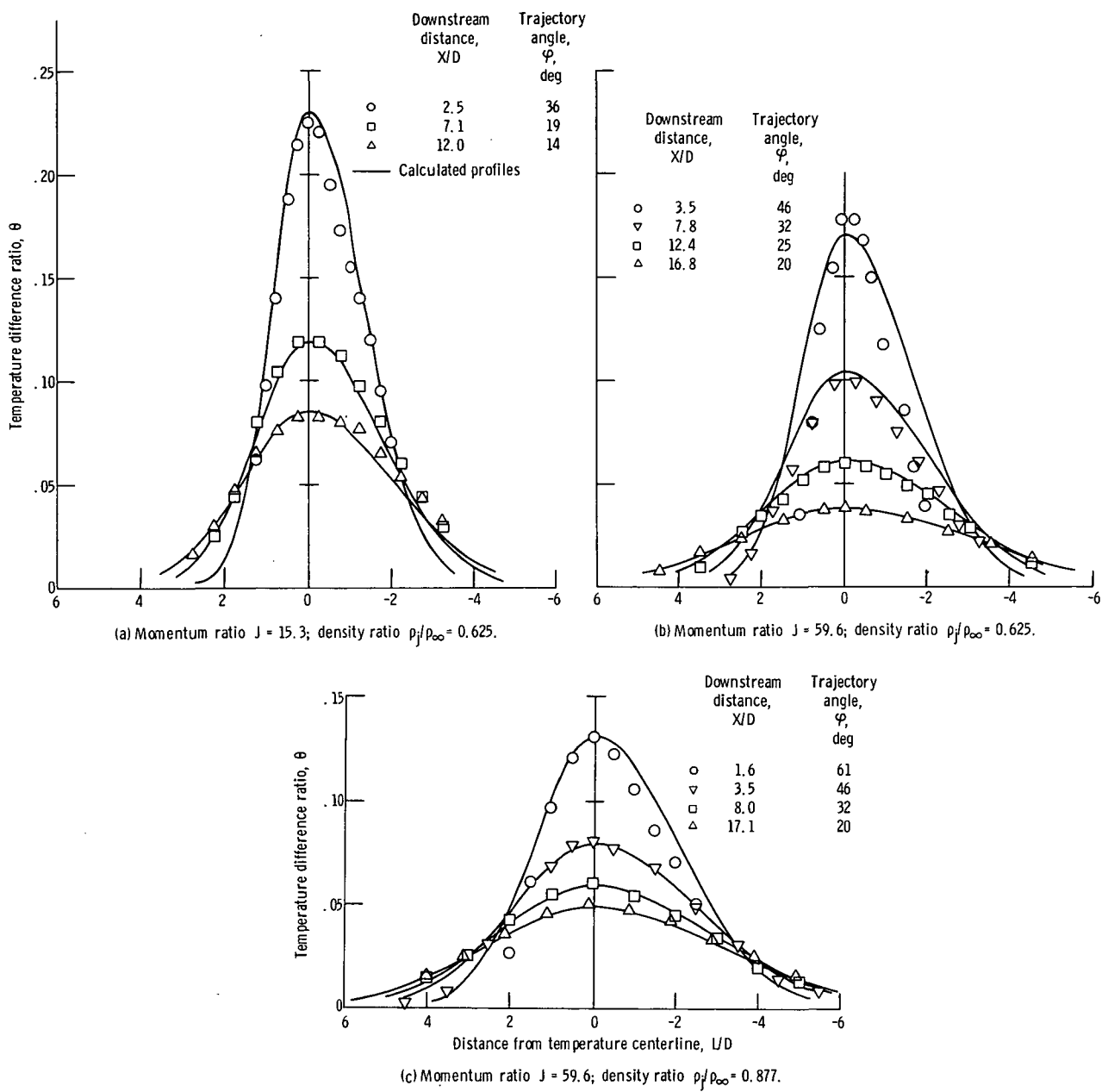


Figure 9. - Temperature profiles in planes normal to velocity trajectory for various momentum ratios J and density ratios p_f/p_∞ .

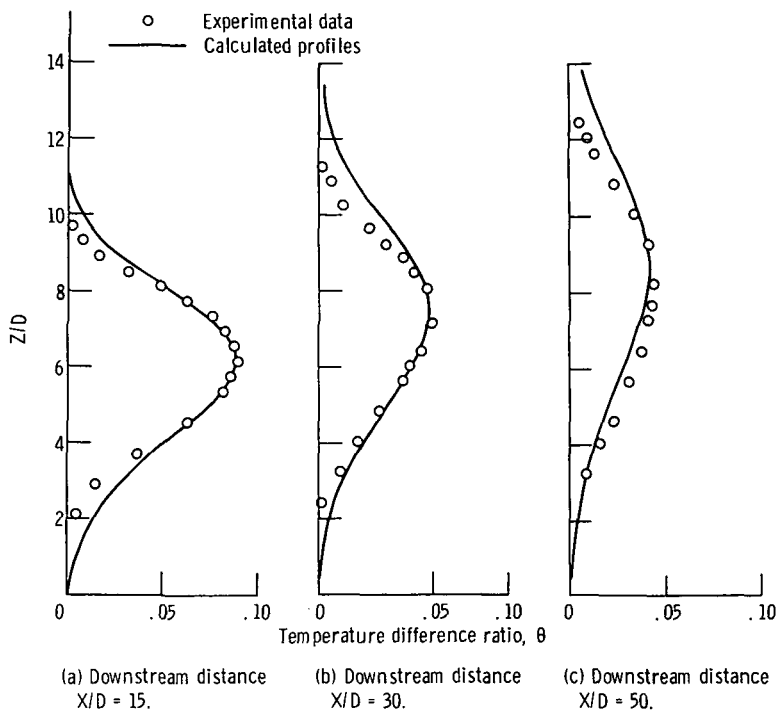


Figure 10. - Comparison of calculated and experimental vertical temperature profiles for momentum ratio $J = 15.3$ and density ratio $p_f/p_\infty = 0.788$.

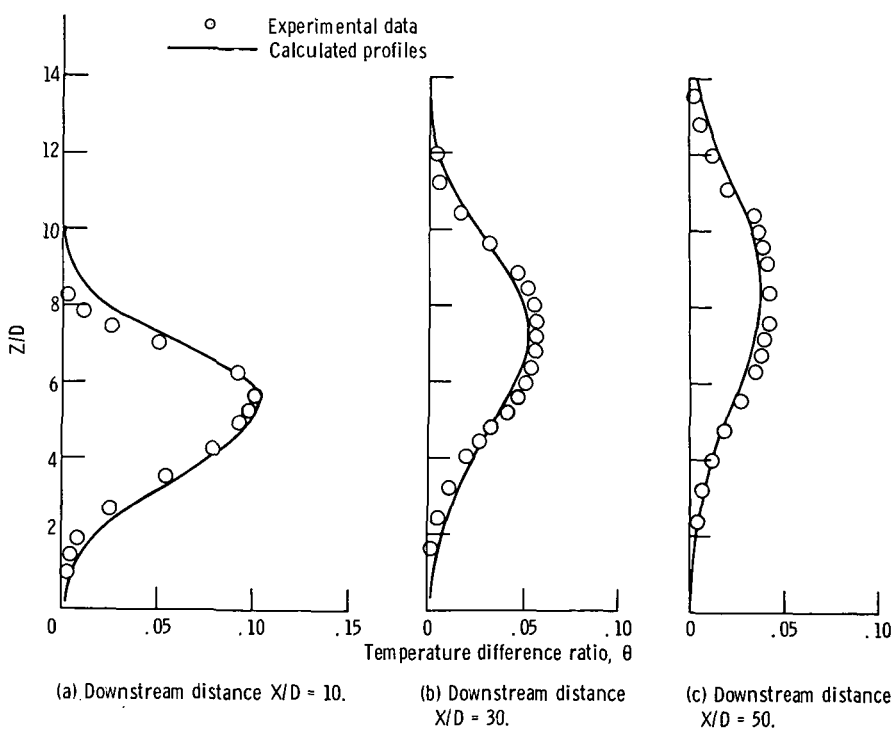


Figure 11. - Comparison of calculated and experimental vertical temperature profiles for momentum ratio $J = 15.3$ and density ratio $p_f/p_\infty = 0.690$.

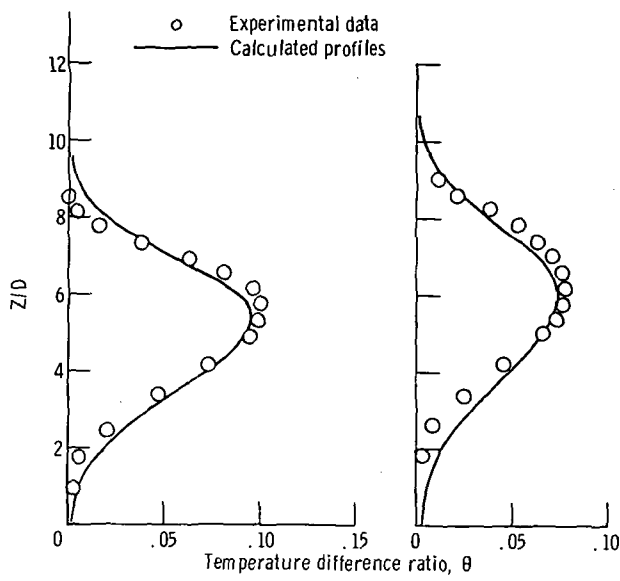


Figure 12. - Comparison of calculated and experimental vertical temperature profiles for momentum ratio $J = 15.3$ and density ratio $\rho_1/\rho_\infty = 0.625$.

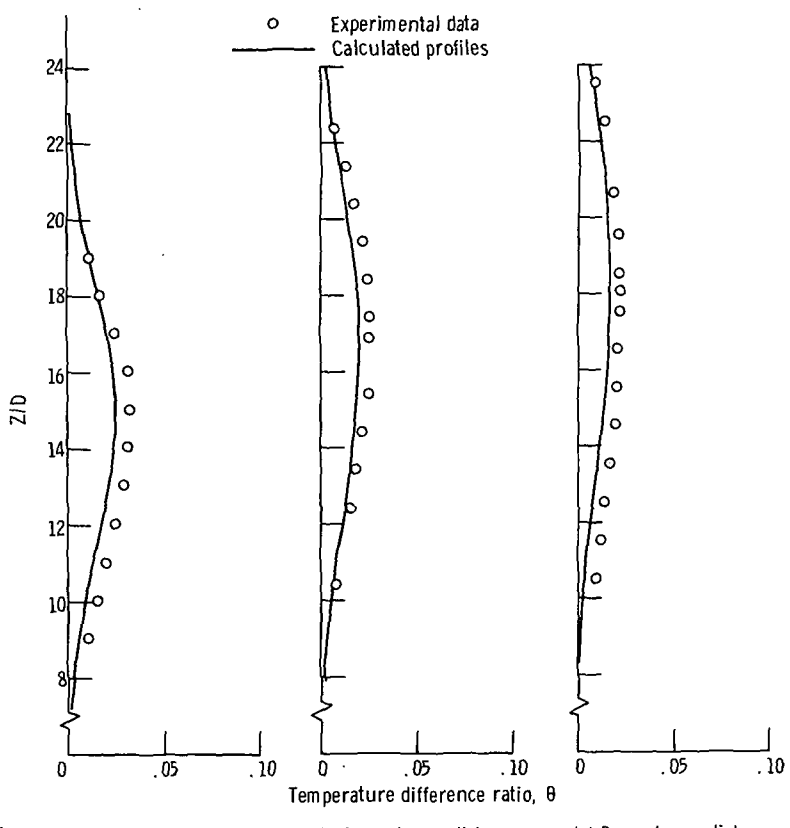


Figure 13. - Comparison of calculated and experimental vertical temperature profiles for momentum ratio $J = 59.6$ and density ratio $\rho_1/\rho_\infty = 0.625$.

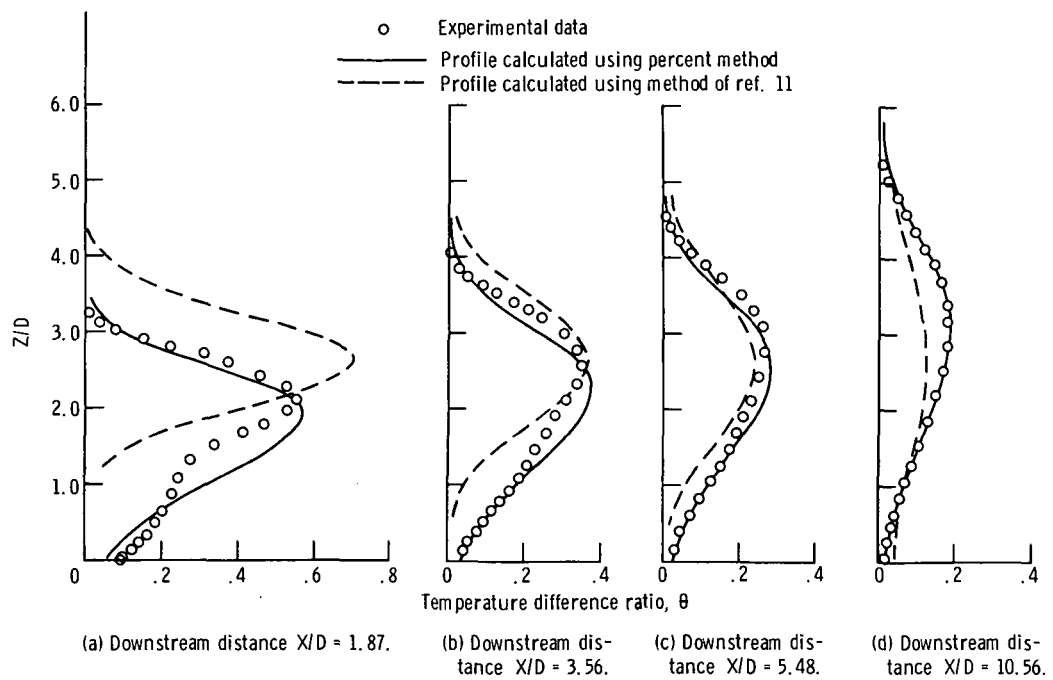


Figure 14. - Comparison of vertical temperature profiles calculated using present method with profiles calculated using method of reference 11, and experimental data for momentum ratio $J = 4.74$ and density ratio $\rho_j/\rho_\infty = 0.843$ from reference 9.

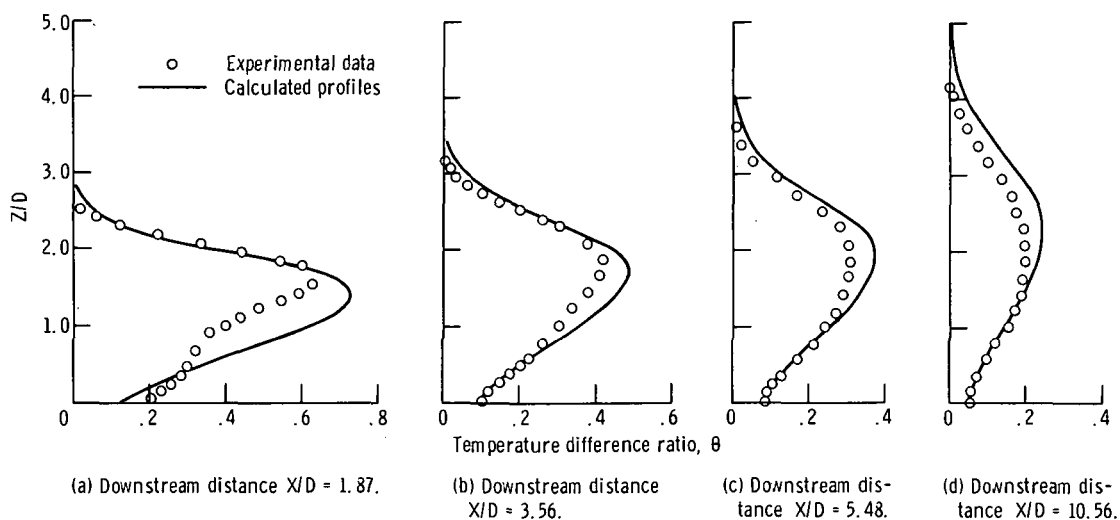
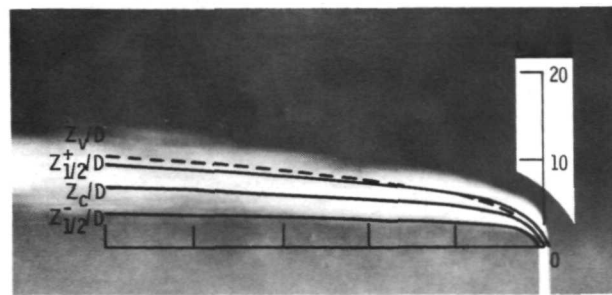
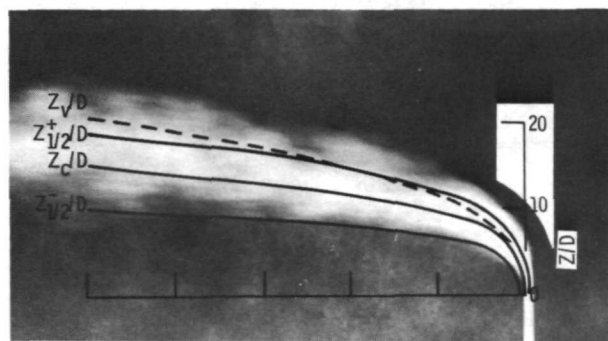


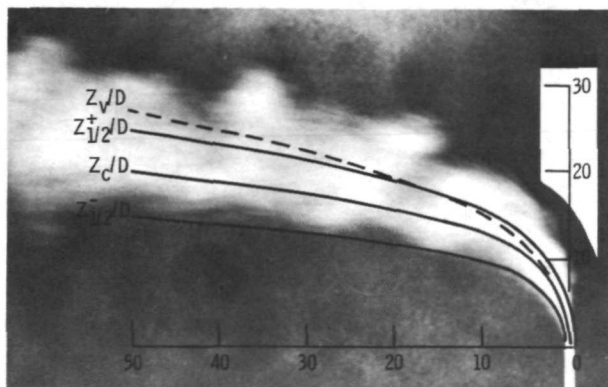
Figure 15. - Comparison of vertical temperature profiles calculated using present method with experimental data for momentum ratio $J = 2.67$ and density ratio $\rho_j/\rho_\infty = 0.843$ from reference 9.



(a) Momentum ratio $J = 10$.



(b) Momentum ratio $J = 40$.



Downstream distance, X/D

(c) Momentum ratio $J = 70$.

Figure 16. - Comparison of velocity trajectory Z_v/D , temperature centerline Z_c/D , and half-width trajectories $Z_{1/2}^+/D$ and $Z_{1/2}^-/D$ with smoke photographs for various momentum ratios J .

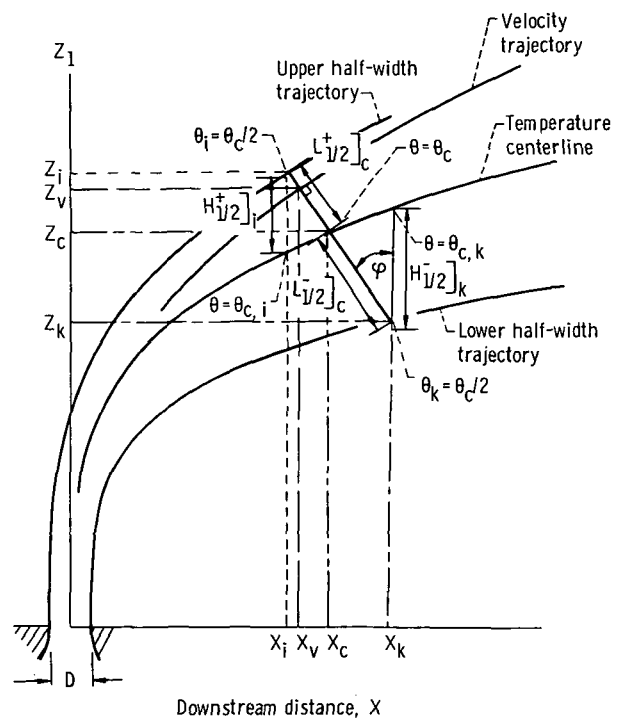


Figure 17. - Parameters for relating profiles normal to velocity trajectory to vertical profiles.

NATIONAL AERONAUTICS AND SPACE ADMINISTRATION
WASHINGTON, D.C. 20546

OFFICIAL BUSINESS
PENALTY FOR PRIVATE USE \$300

FIRST CLASS MAIL

POSTAGE AND FEES PAID
NATIONAL AERONAUTICS AND
SPACE ADMINISTRATION



NASA 451

POSTMASTER: If Undeliverable (Section 158
Postal Manual) Do Not Return

"The aeronautical and space activities of the United States shall be conducted so as to contribute . . . to the expansion of human knowledge of phenomena in the atmosphere and space. The Administration shall provide for the widest practicable and appropriate dissemination of information concerning its activities and the results thereof."

— NATIONAL AERONAUTICS AND SPACE ACT OF 1958

NASA SCIENTIFIC AND TECHNICAL PUBLICATIONS

TECHNICAL REPORTS: Scientific and technical information considered important, complete, and a lasting contribution to existing knowledge.

TECHNICAL NOTES: Information less broad in scope but nevertheless of importance as a contribution to existing knowledge.

TECHNICAL MEMORANDUMS: Information receiving limited distribution because of preliminary data, security classification, or other reasons.

CONTRACTOR REPORTS: Scientific and technical information generated under a NASA contract or grant and considered an important contribution to existing knowledge.

TECHNICAL TRANSLATIONS: Information published in a foreign language considered to merit NASA distribution in English.

SPECIAL PUBLICATIONS: Information derived from or of value to NASA activities. Publications include conference proceedings, monographs, data compilations, handbooks, sourcebooks, and special bibliographies.

TECHNOLOGY UTILIZATION PUBLICATIONS: Information on technology used by NASA that may be of particular interest in commercial and other non-aerospace applications. Publications include Tech Briefs, Technology Utilization Reports and Technology Surveys.

Details on the availability of these publications may be obtained from:

SCIENTIFIC AND TECHNICAL INFORMATION OFFICE

NATIONAL AERONAUTICS AND SPACE ADMINISTRATION

Washington, D.C. 20546